



Low-cost structured alginate-immobilized bentonite beads designed for an effective removal of persistent antibiotics from aqueous solution

Maria Yuliana^{a,*}, Suryadi Ismadji^{a,b}, Jenni Lie^a, Shella Permatasari Santoso^{a,b},
Felycia Edi Soetaredjo^{a,b}, Gladdy Waworuntu^c, Jindrayani Nyoo Putro^a,
Christian Julius Wijaya^{a,d}

^a Department of Chemical Engineering, Widya Mandala Surabaya Catholic University, Kalijudan 37, Surabaya, 60114, Indonesia

^b Department of Chemical Engineering, National Taiwan University of Science and Technology, 43, Keelung Rd., Sec. 4, Taipei, 10607, Taiwan

^c Faculty of Medicine, Widya Mandala Surabaya Catholic University, Pakuwon City, Surabaya, 60112, Indonesia

^d Department of Chemical Engineering, Faculty of Industrial Technology and Systems Engineering, Institut Teknologi Sepuluh Nopember, Keputih Sukolilo, Surabaya, 60111, Indonesia

ARTICLE INFO

Keywords:

Antibiotics
Doripenem
Adsorption
Alginate-immobilized bentonite beads
Facile strategy
Wastewater treatment

ABSTRACT

The removal of persistent antibiotics from the water bodies can be quite challenging. The present study deals with the removal of doripenem, one of the most stable and persistent antibiotics, from aqueous solution via adsorption technique using the low-cost structured alginate-immobilized bentonite (Alg@iB) beads which can be easily recovered after the process. Alg@iB possesses a porous interior and higher basal spacing compared with the acid-activated bentonite (iB). Its adsorption/desorption isotherm corresponds to type IV IUPAC classification and H4-type hysteresis loops, implying the presence of slit- or plane-shaped pores. The influences of four independent adsorption parameters, e.g., pH, initial doripenem concentrations (m_d), temperature (T), and Alg@iB loading (m_c), on the removal rate of doripenem (Y_d) are investigated. The maximum Y_d (95.8% w/w) is obtained at pH = 5, m_c = 1.4% w/v, T = 50 °C, and m_d = 250 mg/l. The study suggests that the adsorption of doripenem is spontaneous and endothermic. Further analysis using the multi-linear intra-particle diffusion (IPD) model indicates that the rate-governing step in this adsorption process is the physical diffusion from the bulk solution to the boundary layer of Alg@iB. However, the mechanism study also considers the chemical hydrogen binding between the hydronium ions of Alg@iB and hydroxyl groups of doripenem as one of the driving forces that promote adsorption. Alg@iB shows good reusability with $Y_d > 90\%$ w/w up to five adsorption cycles. Based on the study, the Alg@iB beads exhibit excellent affinity to doripenem, indicating that an effective doripenem removal can be achieved using this sorbent material.

1. Introduction

Doripenem (also known as Doribax) is a synthetic carbapenem antibiotic and structurally related to the class of beta-lactam antibacterial (Greer, 2008; Hilas et al., 2008). It has been approved by the United States Food and Drug Administration (US FDA) as an essential antibiotic for complicated intra-abdominal infection (Sartelli et al., 2017) which is one of the major contributors to non-trauma deaths caused by severe septic shock and multi-organ dysfunction due to pathogens (e.g., aerobic/anaerobic bacteria, and fungi) (Blot et al., 2019; Blot and De Waele, 2005; Sakr et al., 2018; Vincent et al., 2016). Doripenem possesses activity against both gram-positive bacteria

(Greer, 2008) and the highly resistant gram-negative pathogens, such as *Pseudomonas aeruginosa* (Hilas et al., 2008). It has greater stability in an aqueous solution than the prior components in the carbapenem class, e.g., imipenem, meropenem, and ertapenem. This allows the drug to be infused for more than 4 h, which is beneficial for the treatment of intractable and complicated infections (Greer, 2008; Mazzei, 2010). On the other hand, its high stability induces difficulties for its removal from the aqueous solution. Only 15% of the given dose of doripenem is metabolized and released as an inactive metabolite during the drug administering process, while, around 70% is eliminated in the urine as an unchanged drug (Greer, 2008) which then ends up in a substantial amount of difficult-to-treat doripenem-containing wastewater. The improper disposal and incomplete treatment of antibiotics-containing

* Corresponding author.

E-mail address: mariayuliana@ukwms.ac.id (M. Yuliana).

<https://doi.org/10.1016/j.envres.2021.112162>

Received 1 August 2021; Received in revised form 28 September 2021; Accepted 29 September 2021

Available online 2 October 2021

0013-9351/© 2021 Elsevier Inc. All rights reserved.

Abbreviations

Alg	Alginate
Alg@iB	Alginate-immobilized bentonite composite beads
AOPs	Advanced oxidation processes
iB	Industrial bentonite
IPD	Intra-particle diffusion

wastewater may enter the environment and pollute water bodies (Peng et al., 2016; Ternes et al., 2004). This triggers the developed resistance of the pathogenic bacteria and leads to the mutagenic and genotoxic effects on aquatic organisms as well as humans (Tonucci et al., 2015). Therefore, it is imperative to remove antibiotics from the aqueous solutions in order to minimize their contact with the environment and living communities.

Conventional wastewater treatments can only partially remove this emerging and persistent doripenem. While, advanced methods including the membrane filtration and advanced oxidation processes (AOPs) resulted in high removal efficiency (higher than 90%) (Huber et al., 2005; Košutić et al., 2007). However, both techniques are limited by the expensive cost and severe operating conditions. AOPs require a substantial number of supporting chemicals, which generates secondary pollution and the demand for complicated separation processes. Recently, many studies report the utilization of adsorption techniques to remove various antibiotics (Mousavi and Janjani, 2020; Peng et al., 2016; Yu et al., 2020; Zeng et al., 2018). This method is considered as an effective method to treat wastewater containing antibiotics due to its simplicity, high efficiency, and non-toxic nature. The powdered activated carbon and graphene oxide have been reported to remove various quinolone antibiotics (Fu et al., 2017) and tetracycline in the water (Gao et al., 2012), respectively. Mousavi and Janjani (2020) also reviewed the performance of the walled-, double-walled-, multi-walled-carbon nanotubes to remove the antibiotics from an aqueous solution. However, these carbon-based adsorbents require a relatively high production cost, which is not suitable for industrial practices.

Bentonite is one of the most abundant natural clay mineral and a low-cost adsorbent, characterized by the lamellar and microporous structures, low hydraulic conductivity, and good swelling capacity (Chen et al., 2012; Tan and Ting, 2014). Naturally, it consists of montmorillonite as the major constituent. It generally possesses only a moderate adsorption capacity; therefore, several studies have chemically modified various types of pillared bentonite to improve its adsorption capacity for the removal of antibiotics from the aqueous solutions (Genç et al., 2013; Maged et al., 2020; Wang et al., 2020). Despite its wide applications as the adsorbent, bentonite has some important issues and drawbacks that need to be resolved: (1) it forms a stable colloidal suspension in water due to its swelling ability, which promotes high turbidity and difficulties in the recovery of the used clays, (2) its fine particle size induces low filtration rate, pressure loss and may be carried over in the backwash operations. Therefore, the development of a new fabrication technique to modify the improper powdery form of the bentonite, as well as to mitigate the clogging and post-sorption separation process is required to improve its applications in the aqueous system; that is by immobilizing the fine clay minerals into the polymeric matrix. The synergistic properties between the two materials may complement their characteristics and subsequently enable the comprehensive improvement of the adsorption behavior against various pollutants (Auta and Hameed, 2014), post-separation efficiency, and feasibility (Xu et al., 2020). Sodium alginate as one of the most popular natural polymers has attracted wide interest in wastewater treatment for immobilization purposes of powder-type adsorbents due to its non-toxicity, biodegradability, and low-cost properties (Pawar et al., 2020; Tan and Ting, 2014).

Due to the superior properties of bentonite and alginate, the combination of these two low-cost natural resources, is estimated to be able to enhance the adsorption performance, facilitate better recovery and reusability of the used adsorbent. While the alginate-immobilized bentonite composite beads (Alg@iB) have been studied for the removal of heavy metals and organic fertilizers (Ely et al., 2009; Pawar et al., 2016), to date, there is no published report on the detailed performance of Alg@iB for the antibiotics removal. In this study, the feasibility of using Alg@iB as an adsorbent for doripenem is evaluated under the influence of various parameters (e.g., pH, initial concentration of doripenem m_d , temperature T , and Alg@iB loading m_c). The reusability study of the Alg@iB for the doripenem adsorption is also established for five adsorption-desorption cycles, while the adsorption behavior mechanism of the antibiotics into the internal structure of the beads is elucidated using the kinetics and isotherm studies.

2. Materials and methods

2.1. Materials

The industrial bentonite (iB) was obtained from a local supplier in Pacitan, Indonesia. The material was treated with sulfuric acid according to the study of Fabryanty et al. (2017) prior use. Doripenem (C₁₅H₂₄N₄O₆S₂, CAS No.148016-81-3, ≥98% purity) was obtained from Adooq Bioscience (Irvine, CA). The sodium alginate (CAS No. 9005-38-3) and calcium chloride (CaCl₂, CAS No. 10043-52-4, anhydrous with the purity of ≥97%) were purchased from Sigma-Aldrich (Germany), while the other reagents, e.g., hydrogen peroxide (H₂O₂, CAS No. 7722-84-1, 35% purity), sodium chloride (NaCl, CAS No. 7647-14-5, ≥99.5% purity), sodium hydroxide (NaOH, CAS No. 1310-73-2, 99–100% purity), and sulfuric acid (H₂SO₄, CAS No. 7664-93-9, ≥98% purity) were supplied by Merck (Germany). All reagents were of analytical grade and directly used as received.

2.2. Preparation and characterization of Alg@iB beads

An iB-alginate suspension (2% w/v alginate and 2% w/v iB) was first prepared by (1) dispersing 2 g iB in 50 ml deionized (DI) water under continuous stirring of 500 rpm in one beaker glass; (2) dissolving 2 g of alginate in 50 ml DI water in a separate beaker glass; and (3) mixing the above two solutions for 4 h via vigorous stirring-ultrasonic processing. The mixture was then transferred to a burette equipped with a pipette tip, and it was slowly dropped into a 4% w/v CaCl₂ solution which was continuously stirred to form the Alg@iB beads. The resulting beads were allowed to harden in the CaCl₂ solution for another 3 h to enhance their mechanical strength and subsequently filtered, rinsed with DI water until the pH reaches 7.0, and dried to constant weight at 40 °C. The same procedures were employed to prepare the plain alginate (Alg) beads, substituting iB with DI water.

The iB, Alg, and Alg@iB beads were characterized by several physicochemical analysis techniques, including scanning electron microscopy (SEM), X-Ray powder diffraction (XRD), nitrogen (N₂) sorption, Fourier transform infrared (FTIR), and point-of-zero-charge (pH_{pzc}). The SEM micrographs were obtained by SEM JEOL JSM-6500F (Jeol Ltd., Japan). The respective voltage and working distance of the analysis are set between 10 and 15 kV and 9.4–10.9 mm, respectively. The XRD analysis was conducted using an X'PERT Panalytical Pro X-Ray diffractometer (Philips-FEI, Netherlands) at 40 kV and 30 mA tube current with the 2θ ranges from 2° to 70°. The monochromatic Cu Kα₁ radiation (λ) is set at a wavelength of 0.154 nm. The textural properties (e.g., specific surface area, S_{BET}, and pore volume, V_p) of iB and Alg@iB beads were measured at a temperature of 77 K using a Micromeritics ASAP 2010 sorption analyzer. The FTIR spectra were acquired using Shimadzu FTIR 8400s from 400 to 4000 cm⁻¹. The point-of-zero-charge (pH_{pzc}) of Alg@iB was measured by Malvern Zetasizer Nano Z (Malvern Panalytical Ltd., UK) with the pH range of 2–11.

2.3. Adsorption of doripenem onto Alg@iB

The experimental runs of the doripenem adsorption were conducted in a series of flasks with a range of pH (2, 5, 8, 11), initial doripenem concentrations ($m_d = 100, 150, 200, 250$ mg/l), temperature ($T = 30, 40, 50$ °C), and Alg@iB loading ($m_c = 0.2, 0.4, 0.6, 0.8, 1.0, 1.2, 1.4\%$ w/v). In this study, all experiments were carried out in a 50 ml doripenem solution sample. Initially, the effect of pH was studied at $m_d = 250$ mg/l, $T = 30$ °C, and $m_c = 1.4\%$ w/v. The pH of the sample was adjusted using 2 N H₂SO₄ and 1 N NaOH solutions before the addition of Alg@iB. The adsorption system was then heated to the desired T , and subsequently, the measured amount of dried Alg@iB beads was immersed into the solution. The system was maintained isothermally under continuous agitation for 180 min (this duration was obtained from the study of adsorption kinetics – section 2.5) before phase separation. After the complete sorption process, the Alg@iB beads were filtered out from the solution and the concentration of doripenem in the supernatant was analyzed by Shimadzu UV-Vis spectrophotometer 2600 (Shimadzu, Japan). The removal rate of doripenem Y_d was calculated using equation (1) below:

$$Y_d(\% \text{ w / w}) = \frac{100 (C_0 - C_f)}{C_0} \quad (1)$$

Where, C_0 and C_f are the initial and final concentrations of doripenem in the solution (mg/l), respectively. Further experiments to monitor the influence of m_d , T , and m_c on Y_d were then performed using the same procedure at optimum pH. The operating condition giving the highest Y_d was used for the reusability study (section 2.4).

2.4. Reusability study of Alg@iB

The reusability test was conducted for 5 identical adsorption – regeneration – desorption cycles. The Alg@iB beads were regenerated by acid immersion at two different temperatures (30, 40 °C). The used beads were immersed in 0.2 N H₂SO₄ solution for 120 min at a certain temperature and kept under a constant stirring rate of 150 rpm. The regenerated Alg@iB beads were then rinsed using DI water until no more doripenem leached out (verified by the UV-Vis spectrophotometric analysis of the rinsing water), vacuum dried at 40 °C, and reused for the next adsorption studies. All experimental runs were carried out thrice to confirm the results.

2.5. The kinetics and isotherm studies

In the kinetics study, the doripenem solution ($m_d = 250$ mg/l) was introduced into a series of beaker glass, adjusted to pH = 5 using H₂SO₄ and NaOH solutions, and heated to a certain temperature ($T = 30, 40, 50$ °C). Then, the Alg@iB beads were added to the solution with $m_c = 1.4\%$ w/v. The mixture was stirred to keep the system homogenous. Each beaker glass was collected at different time intervals, and the concentration of doripenem in the supernatant was measured. The adsorption capacity at a certain time (Q_t) can be determined using equation (2), where C_0 and C_t correspond to the initial doripenem concentration and its concentration at time t (mg/l), w_c defines the mass of the Alg@iB (g), and V is the volume of doripenem solution (l).

$$Q_t(\text{mg / g}) = \frac{V (C_0 - C_t)}{w_c} \quad (2)$$

The uptake data obtained from section 2.3 was used to conduct the isotherm studies, where the adsorption capacity at equilibrium (Q_e) can be expressed as follows.

$$Q_e(\text{mg / g}) = \frac{V (C_0 - C_e)}{w_c} \quad (3)$$

The term of C_e in equation (3) stands for the equilibrium

concentration of doripenem in the solution (mg/l). The computed equilibrium data were fitted to several isotherm models, including Langmuir, Freundlich, Temkin, and Dubinin-Radushkevich (D-R). The resulting isotherm parameters were then employed to analyze the Gibbs free energy (ΔG°), enthalpy (ΔH°), entropy (ΔS°) of the adsorption process. These three thermodynamics properties may be used to further elaborate the adsorption mechanism.

3. Results and discussions

3.1. Characteristics of Alg@iB

Fig. 1 depicts the micrographs of acid-treated iB (a), Alg (b), and Alg@iB (c–d). The captured topographies of the three samples show a significant difference, where the surface of acid-treated iB is flakey, quite rigid, and smooth with an irregular shape, while the morphology of Alg reveals a rough and compact nature. The image of Alg@iB displays the formation of pores on the surface of the composite. The incorporation of bentonite in the adsorbent is highly beneficial because it allows the interior surface of the adsorbent to be porous (Tan and Ting, 2014), and more exposed to the doripenem. This facilitates the permeation of water into the inner structure of Alg@iB, and therefore, leads to the higher removal of doripenem.

The nitrogen sorption of iB and Alg@iB are plotted in Fig. 2a. Notably, their isotherms correspond to type IV in the IUPAC classification. The loop characteristics of all samples follow the H4-type hysteresis, usually observed for samples containing slit- or plane-shaped pores. These adsorption/desorption profiles confirm the presence of the layered clay materials with complex interiors (non-uniform micropores and mesopores). The important textural properties of iB and Alg@iB are obtained from the BET isotherm. While the specific surface area and pore volume of iB are found to be 257.4 m²/g and 0.364 cm³/g, respectively, the corresponding values of both parameters for Alg@iB are 291.1 m²/g and 0.297 cm³/g. The smaller pore volume and slimmer hysteresis loop (Fig. 2a) are monitored in Alg@iB as compared with that in iB, suggesting that some pores are occupied with the Alg after the immobilization. The active sites crosslinked with Alg are also responsible for the declining value of pore volume of Alg@iB. However, the results also reveal an increase in the surface area of Alg@iB. This is probably attributed to the swelling nature of bentonite upon contact with water (Tan and Ting, 2014).

To verify the formation of the Alg@iB composite, the surface functional groups of iB and Alg@iB are analyzed. The functional groups shown by the Alg@iB composite are quite similar to iB, with the characteristic peaks shown in Fig. 2b. The prominent peak at 1087 cm⁻¹ and 1040 cm⁻¹ is correlated to the Si–O stretching vibration of iB and Alg@iB, respectively. The asymmetric stretching vibration of the carboxyl group is monitored at 1656 cm⁻¹ for iB; this peak is shifted to 1637 cm⁻¹ for Alg@iB. Minor bands at 521 cm⁻¹ for iB and 474–546 cm⁻¹ for Alg@iB represent the Si–O–Si and Si–O–Al bending vibrations. The broad peak at 3128 - 3145 cm⁻¹ correlates to the stretching of the hydroxyl group, while the bands at 3615–3635 cm⁻¹ show the (Si, Al) – OH stretching vibration. As seen from Fig. 2b, the changes in the FTIR bands of Alg@iB is observed at 1421 cm⁻¹. This corresponds to the symmetric stretching vibration of the carboxyl (-COO-) group and is contributed to the alginate moiety. The new peak and few alterations in the spectra indicate the interaction between sodium alginate and iB in th composite, confirming the formation of Alg@iB.

Fig. 2c represents the diffraction pattern of Alg, iB, and Alg@iB. The amorphous structure is seen from the XRD pattern of Alg. Meanwhile, the characteristic peaks of montmorillonite (M, ICDD #13–0259 and #29–1498), kaolinite (K, ICDD #06–0221 and #01–0527), and quartz (Q, ICDD #03–0419) are identified at similar 2θ value in both iB and Alg@iB. Notably, the merging of iB and alginate affects the crystallinity of bentonite, indicated by a significant shift in '001' diffraction peak from $2\theta = 6.55^\circ$ to $2\theta = 5.86^\circ$. This result implies the increase in the

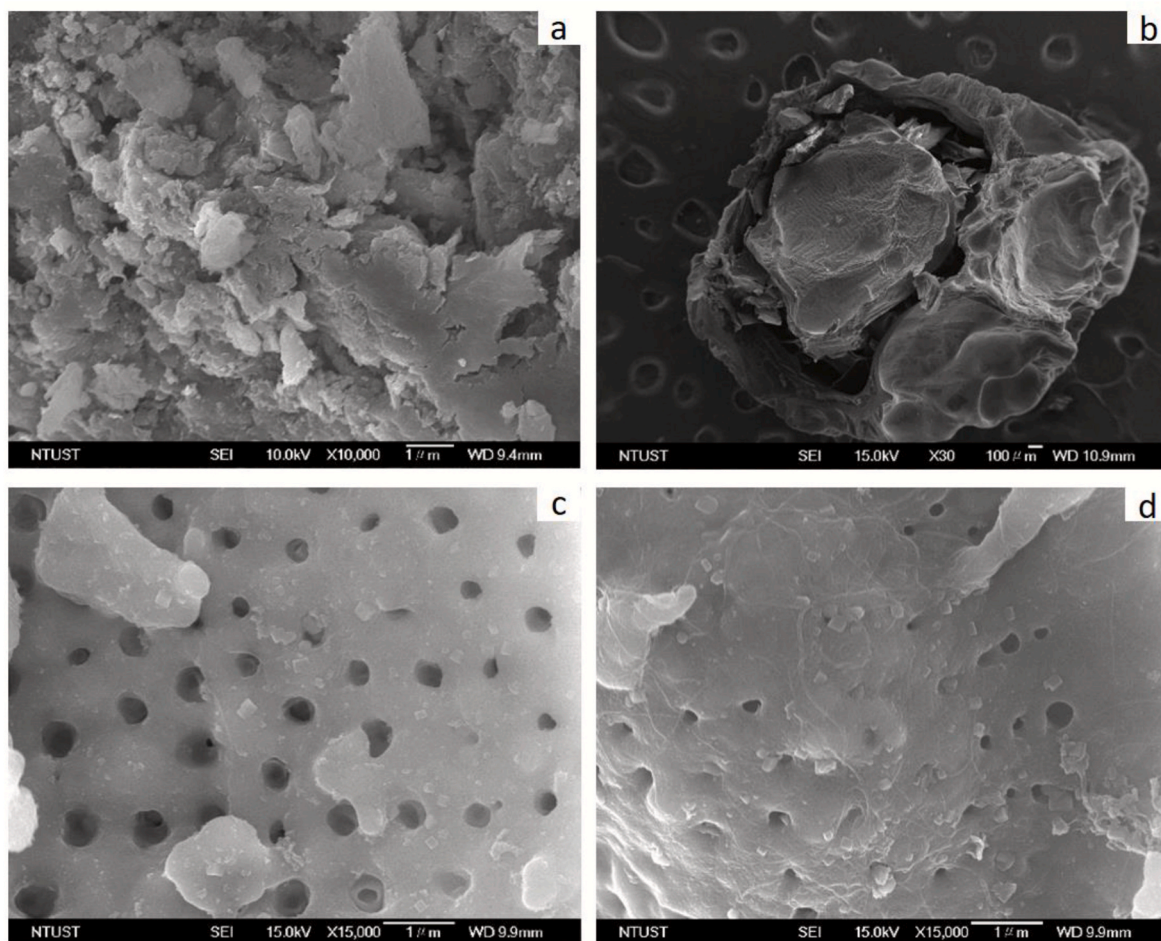


Fig. 1. SEM images of (a) iB, (b) Alg, (c-d) Alg@iB

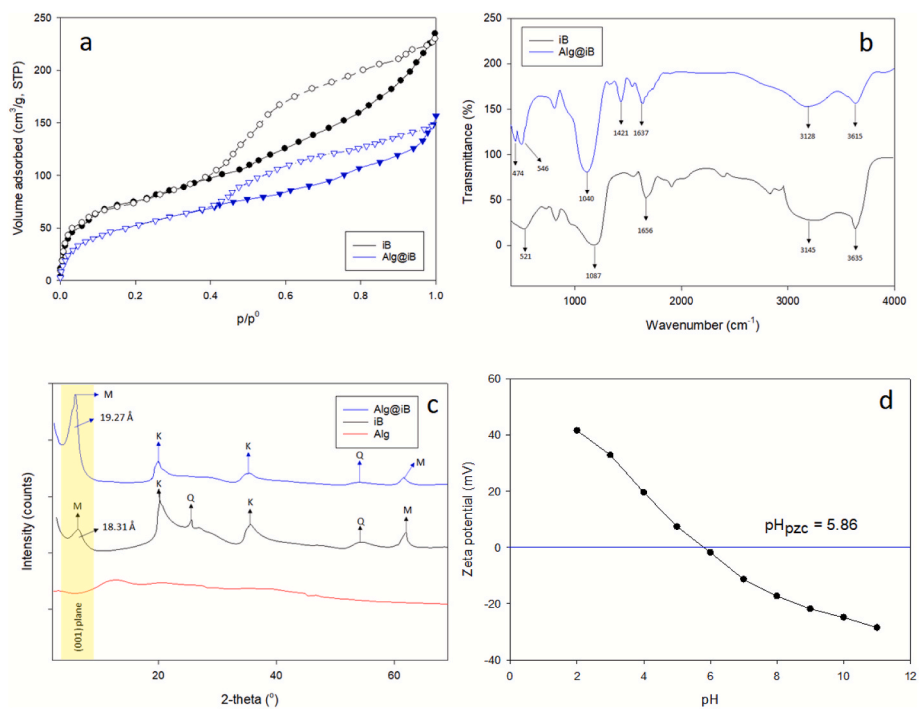


Fig. 2. (a) N₂ sorption, (b) FTIR spectra, (c) XRD pattern, and (d) pHP_{zpc} of Alg@iB

basal spacing from 18.31 Å in iB to 19.27 Å in Alg@iB, which is likely contributed by the increase in the interlayer region of Alg@iB due to the presence of immobilized Alg.

The pH_{pzc} of Alg@iB is obtained at a neutral region (Fig. 2d), with a value of 5.86. The composites are positively charged at pH lower than pH_{pzc} due to the occurrence of excessive hydronium (H^+) ions which further causes the adsorbent to protonate. Meanwhile, at $pH > pH_{pzc}$, the excess hydroxyl (OH^-) ions provoke the deprotonation of the H^+ and lead to the charge-shifting of the Alg@iB to the negative side.

3.2. The influence of the adsorption parameters on the removal of doripenem

In most cases, the adsorption performance of an adsorbent is influenced by the change in the solution pH, as pH alters the total surface charge of the system and the electrostatic interaction between the adsorbent and adsorbate. As previously shown in Fig. 2d, the pH_{pzc} value of the Alg@iB beads is observed at 5.86. This implies that the surface of Alg@iB is positively charged when the solution pH is less than pH_{pzc} , and vice versa.

The experimental results show that the removal of doripenem fluctuates along with the pH, where the removal magnitude increases from 69.03% (w/w) to 90.07% (w/w) when the pH elevates from pH = 2 to pH = 5. Subsequently, the removal rate of doripenem decreases to 79.49% (w/w) and 70.36% (w/w) when the pH level increases to pH = 8 and pH = 11, respectively. These results demonstrate that the adsorption of doripenem is limited to a pH lower than pH_{pzc} ($pH < 5.86$), with the highest removal rate at pH = 5. Zeng et al. (2018) studied that at $pH < 7$, most of the antibiotics (including doripenem) are partially protonated and found as a mixture of zwitterionic and cationic species in the solution. The number of cationic species is also reported to escalate significantly along with the decrease in pH value. This provokes the occurrence of the electrostatic repulsion between the cationic species of doripenem and positively charged Alg@iB and subsequently reduces the removal rate of doripenem (Shyam et al., 2013). Due to this reason, our study observes a low removal rate of doripenem at an extremely acidic condition (pH = 2). A similar phenomenon also happens at $pH > 7$, as the deprotonated antibiotics and the negatively-charged Alg@iB are repulsive towards each other, reducing the adsorption ability of Alg@iB.

At a constant pH (pH = 5), Fig. 3 presents the removal of doripenem Y_d at various T , m_d , and m_c . The maximum Y_d is obtained at adsorbent loading $m_c = 1.4\%$ w/v, temperature $T = 50^\circ C$, and initial doripenem concentration $m_d = 250$ ppm. As seen in the figure, T remarkably influences the adsorption rate of doripenem onto the surface of Alg@iB. This study sees a prominent increase in the reduction of doripenem from the aqueous solution when T is elevated from the lowest ($30^\circ C$) to the highest level ($50^\circ C$). The diffusion rate of the adsorbate through the boundary layer of the Alg@iB surface escalates with the temperature rise, which is mainly attributed to the lower viscosity of the solution (Chowdhury et al., 2011). Besides, a higher T enhances the mobility and kinetic energy of the adsorbate, causing intense collisions between particles. This eases the adsorption process to achieve its activation energy, and as a result, the amount of doripenem uptaken into Alg@iB beads increases along with the temperature rise.

Notable from Fig. 3, m_d also plays a major role in the increase of the doripenem removal rate, where higher m_d results in the higher Y_d at constant m_c and T . This is likely due to the increased chance of contact between the antibiotics and Alg@iB in solutions with higher m_d (Tan and Ting, 2014), accelerating the collision between both adsorbent and adsorbate and subsequently, resulting in a higher adsorption capacity. Pawar et al. (2016) and Xu et al. (2020) also reported that the resistance at the mass transfer interface between the adsorbent surface and aqueous solution is also overcome at higher concentrations. However, an insignificant increase of the uptake of doripenem by Alg@iB is also observed when m_d is escalated from 200 mg/l to 250 mg/l, which indicates that all binding sites on the Alg@iB are fully occupied with the

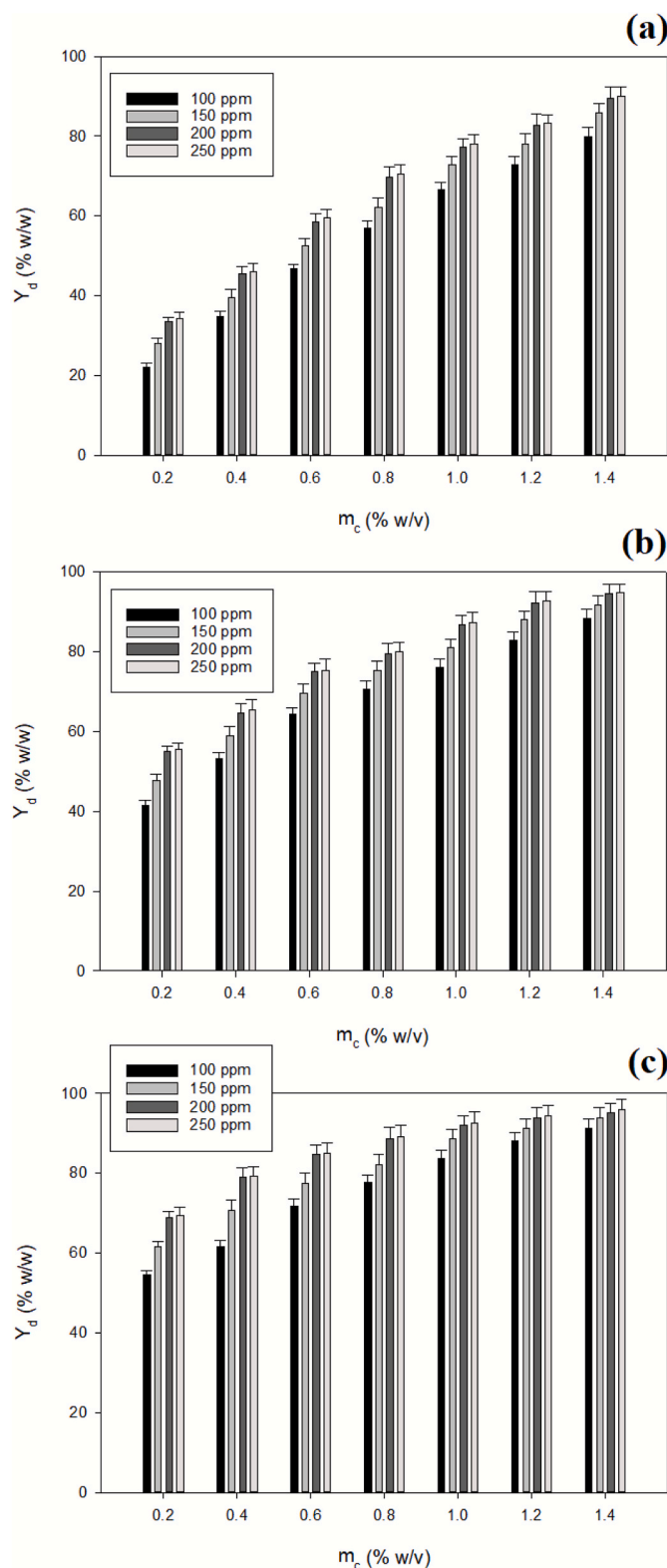


Fig. 3. The removal of doripenem (Y_d) varied with the initial doripenem concentration (m_d) and Alg@iB loading (m_c) at (a) $T = 30^\circ C$, (b) $T = 40^\circ C$, (c) $T = 50^\circ C$.

antibiotics at these concentrations.

A similar profile is observed for the effect of various m_c on the removal rate of doripenem. At $T = 30^\circ C$ and within all tested m_d , increasing the value of adsorbent loading from $m_c = 0.2\%$ w/v to $m_c = 1.4\%$ w/v linearly escalates Y_d . Meanwhile, at $T = 40-50^\circ C$, Y_d rises

significantly at the first five doses of Alg@iB ($m_c = 0.2\text{--}1.0\%$ w/v), and elevates gradually thereafter. These results indicate that Y_d is proportional to the number of active sites offered by Alg@iB (Pawar et al., 2020). A slight increase obtained while increasing the Alg@iB loading from $m_c = 1.0\%$ w/v to $m_c = 1.4\%$ w/v is likely because almost 100% removal of doripenem is achieved.

3.3. The kinetics and mechanism study of doripenem adsorption into Alg@iB

Fig. 4 reveals that the sorption capacity of Alg@iB increases significantly in the first 20 min, adsorbing more than 50% of the total doripenem from the aqueous solution. The removal rate of doripenem is relatively slow thereafter, and the equilibrium is reached within 180 min. The same behavior is observed for all temperatures; however, escalating the temperature from 30 °C to 50 °C is monitored to improve the adsorption capacity of Alg@iB by two folds, which could be attributed to the increasing diffusion rate of adsorbate at higher temperatures (Chowdhury et al., 2011).

To evaluate the sorption kinetics of doripenem onto Alg@iB, the following pseudo-first-order (equation (4)), pseudo-second-order (equation (5)), and intra-particle diffusion (IPD, equation (6)) equations are used, where Q_e and Q_t (mg/g) correspond to the amount of doripenem adsorbed on Alg@iB at equilibrium and at a certain adsorption time t (min), k_1 , k_2 , and k_p represent the adsorption constants for pseudo-first-order, pseudo-second-order, and IPD kinetics, respectively. The computed kinetic parameters are presented in Table 1.

$$Q_t = Q_e(1 - e^{-k_1 t}) \quad (4)$$

$$Q_t = \frac{Q_e^2 k_2 t}{(1 + Q_e k_2 t)} \quad (5)$$

$$Q_t = k_p (t^{1/2}) + C \quad (6)$$

Based on the data comparison of the three models (Table 1), pseudo-second-order is better in describing the adsorption behavior of doripenem onto the surface of Alg@iB. The results imply that the chemisorption governs the adsorption more than the physisorption, where the sorption capacity heavily depends on the number of binding sites on the adsorbent. However, with (1) only a slight difference of R^2 between the pseudo-second-order and pseudo-first-order, (2) the linear line passing through the origin, and (2) the higher value of k_1 compared with k_2 , we may also consider IPD as one of the steps controlling the adsorption rate (Ho and McKay, 1999; Simon et al., 2019). Therefore, we use the multi-linear IPD model to break down the adsorption steps (Figs. 4c and 5). The whole adsorbate movement from the aqueous solution to the interior of Alg@iB can be divided into three steps as follows: (1) the diffusion of doripenem molecules from the bulk solution to the external boundary layer of Alg@iB, (2) the intra-particle migration of doripenem from the boundary layer to the inner part of Alg@iB, and (3) the molecules of doripenem chemically embed on the active binding sites of Alg@iB via hydrogen bonding between the hydroxyl arms of doripenem and hydronium ions in the lamellar spacing of Alg@iB; a similar mechanism is observed for all adsorption temperatures. The results show that the adsorption constant of the first step (k_{p1}) is higher than those of the second (k_{p2}) and third (k_{p3}) steps (Fig. 4c), suggesting that the physical diffusion from the bulk solution to the boundary layer is indeed the rate-governing step, followed successively by the IPD and chemical embedding of doripenem on the surface of Alg@iB. An endothermic nature of the sorption process is also monitored from the data presented in Table 1, due to the escalating values of k_1 , k_2 , k_p , and equilibrium adsorption capacity (Q_e) along with the temperature from $T = 30\text{ °C}$ to $T = 50\text{ °C}$.

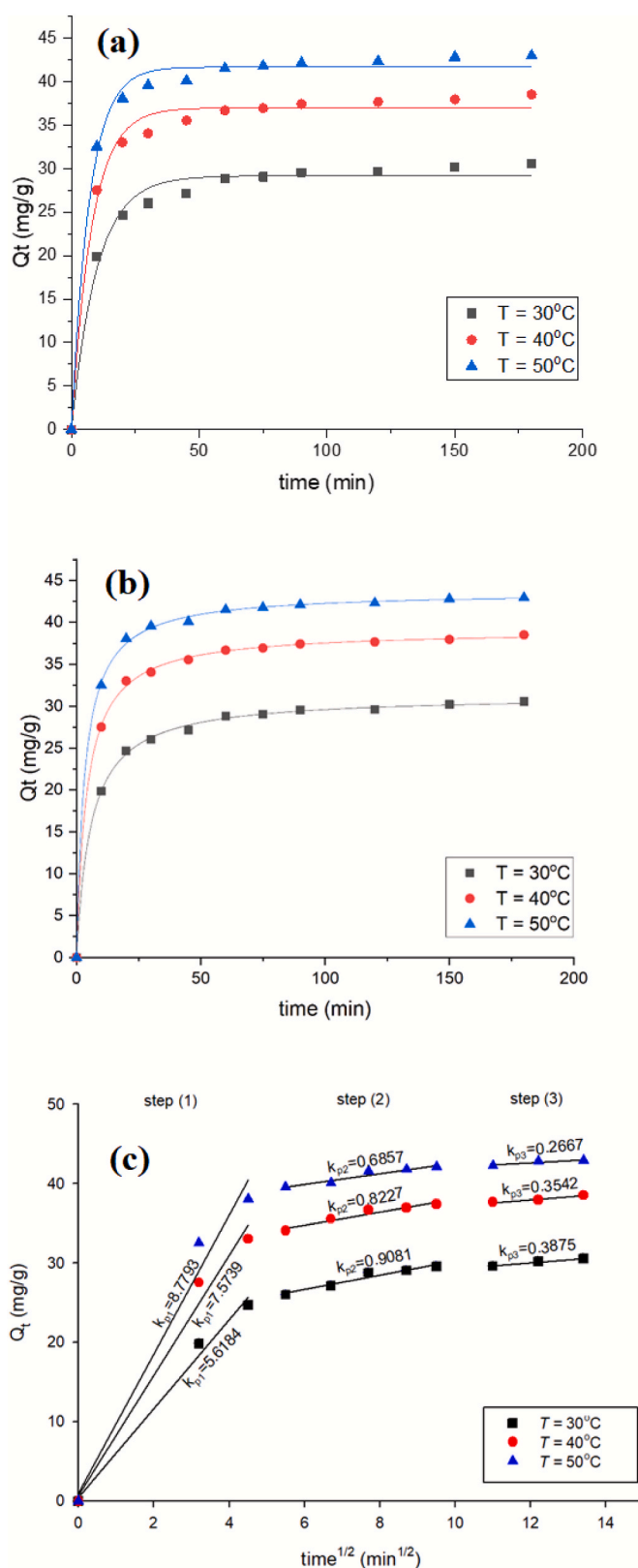


Fig. 4. Adsorption kinetic data of doripenem onto Alg@iB, regressed using (a) pseudo-first order, (b) pseudo-second order, (c) IPD model (pH = 5, $m_d = 250$ mg/l, and $m_c = 1.4\%$ w/v).

Table 1
The computed adsorption kinetic parameters of the doripenem onto Alg@iB

Model	Parameters	Temperature		
		30 °C	40 °C	50 °C
Pseudo-first order	k_1 (g/mg.min)	0.1006	0.1252	0.1423
	Q_e (mg/g)	29.15	36.97	41.67
	R^2	0.9837	0.9892	0.9926
Pseudo-second order	k_2 (g/mg.min)	0.0056	0.0062	0.0069
	Q_e (mg/g)	31.29	39.08	43.66
	R^2	0.9989	0.9994	0.9994
IPD	k_p (mg/g.min ^{1/2})	1.8099	2.1669	2.3550
	C	11.486	16.063	19.059
	R^2	0.6774	0.6142	0.575

3.4. Isotherm study

To obtain insight on the possible sorption mechanism, four isotherm equations (Freundlich, Langmuir, Temkin, and Dubinin-Radushkevich (D-R)) are fitted into the equilibrium data at different temperatures and the developed graphs are presented in Fig. 6. Meanwhile, the calculated parameters and constants are summarized in Table 2. A careful comparison of the four models shows that the adsorption of doripenem onto Alg@iB is best fitted to the Langmuir model and mainly driven by both hydrogen bonding. Fig. 6 also indicates that the experimental and predicted Q_e are similar to each other, confirming the validity of this model to describe the adsorption of doripenem. The conformity of the model towards the Langmuir isotherm suggests that the adsorbate forms a monolayer on the surface of the adsorbent and this sorption happens at particular homogenous sites within the surface of Alg@iB (Rusmin et al., 2015). The escalating value of the Langmuir constant (K_L) along with the temperature from 0.016 L/mg at $T = 30$ °C to 0.043 L/mg at $T = 50$ °C emphasizes the favorability of the sorption process at a higher temperature. The computed $Q_{m(L)}$ is observed to increase from 49.89 mg/g at $T = 30$ °C to 72.11 mg/g at $T = 50$ °C, indicating that the process is endothermic.

The favorability of the sorption based on the Freundlich isotherm is evaluated using the dimensionless $1/n$. Table 2 shows that the $1/n$ value at various temperatures ranges from 0.340 to 0.464, indicating that the adsorption is favorable (Widdyaningsih et al., 2020). Similar to the Langmuir constant, both Freundlich (K_F) and Temkin (K_T) constants also prominently escalate from 30 °C to 50 °C. This verifies the endothermic nature of the sorption process.

Table 2 also lists the heat of sorption (E_T) obtained from the Temkin regression. The values are monitored between 200.7 and 259.29 J/mol at the three temperature levels. Atkins (1999) mentioned that the E_T

value lower than 20 kJ/mol indicates the nature of physical sorption; therefore, the resulting value of E_T supports the physisorption theory previously mentioned in the kinetic study. To confirm the adsorption nature of Alg@iB towards doripenem, the mean sorption energy (E_{D-R}), defined as the free energy transfer of 1 mol of solute from the infinity of surface of the adsorbent, is also computed using the isotherm model of Dubinin-Radushkevich. Chowdhury et al. (2011) stated that when the E_{D-R} value is lower than 8 kJ/mol, the sorption occurs via physical interaction. With all E_{D-R} values at various temperatures lower than 8 kJ/mol (Table 2), they confirm that the physical interaction (bulk diffusion and IPD) governs more than the chemical hydrogen binding during the doripenem migration from the bulk aqueous solution to the surface of the adsorbent (Fig. 5).

Three important thermodynamic parameters, e.g., Gibbs free energy change (ΔG°), enthalpy (ΔH°) and entropy (ΔS°), are listed in Table 3. Spontaneous and favorable adsorption of doripenem onto the surface of Alg@iB is monitored in this study, indicated by the negative values of ΔG° at all tested temperatures. The rising value of ΔG° along with the temperature also suggests a higher affinity of doripenem on Alg@iB at a higher temperature. The endothermic nature is confirmed by the positive value of the enthalpy (40.09 kJ/mol). Meanwhile, the entropy of the adsorption is obtained at 206 J/mol.K, pointing out the increased randomness of doripenem molecules on the surface of Alg@iB at a higher temperature. This enhances the affinity of the doripenem to the binding sites of Alg@iB (Liu and Liu, 2008). Based on the results, the satisfactory removal of doripenem ($Y_d > 90\%$) implies that Alg@iB has a high affinity towards doripenem, and is a potential adsorbent for the removal of doripenem from the aqueous solution.

3.5. Reusability study

The reuse potential of Alg@iB to remove the doripenem from the aqueous solution is investigated for 5 consecutive adsorption and regeneration cycles; the results are shown in Fig. 7. Notable from the figure, the regenerated Alg@iB has generally a reduced adsorptive capacity. The loss of the removal rate is caused by a fewer number of binding sites available in the regenerated Alg@iB, which is likely due to the incomplete removal of the doripenem from the interior of Alg@iB (Santoso et al., 2020).

The results also indicate that the combination of the chemical and mild thermal treatment proves to be a promising regeneration technique, as we observe only a 5.7% decrease in the removal rate of doripenem until the fifth run. Meanwhile, a significant decline (from 95.8 to 83.4% w/w) in the adsorptive rate of doripenem is monitored since the second cycle when the used Alg@iB beads are immersed in the sulfuric

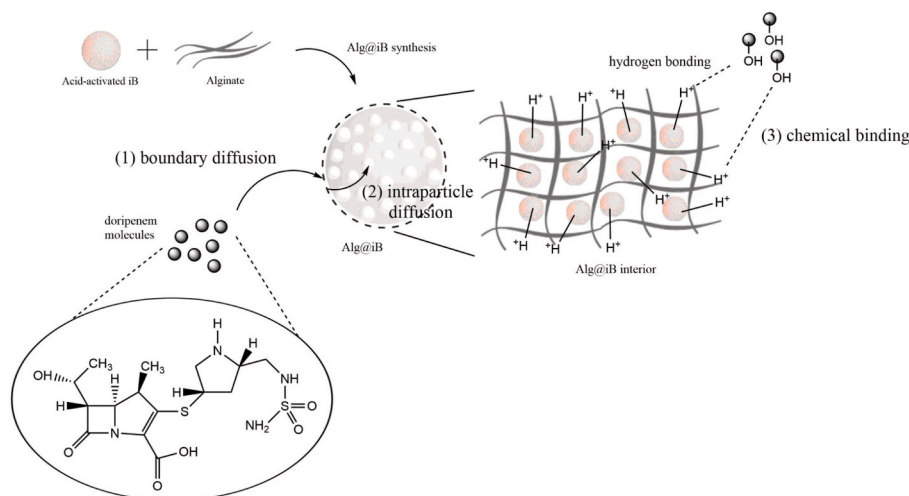


Fig. 5. The adsorption mechanism of doripenem onto the Alg@iB interior.

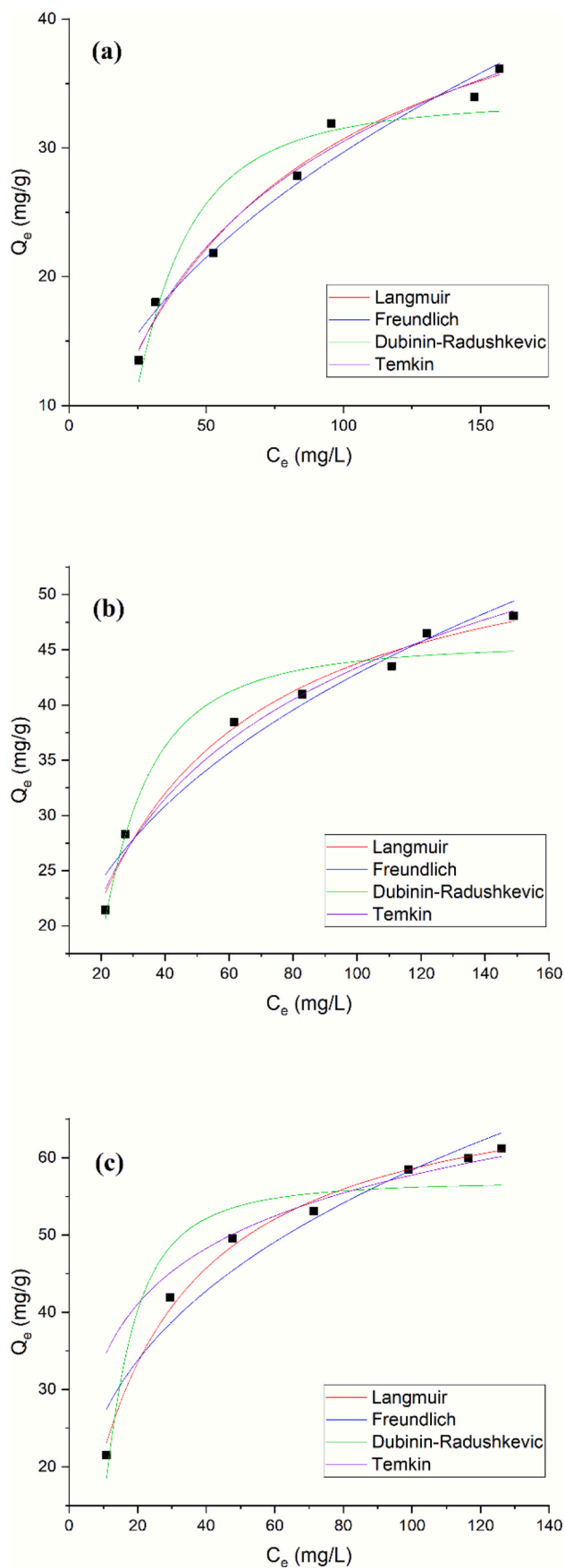


Fig. 6. The fits of four isotherm models on the adsorption equilibrium data of doripenem onto Alg@iB

Table 2

The fitted parameters of isotherm adsorption between doripenem and Alg@iB at pH = 5 and $m_d = 250$ mg/l.

Isotherm	Parameters	Temperature (K)		
		303	313	323
Freundlich	K_F (mg/g) (L/mg) ^{1/n}	3.497	8.222	12.196
	1/n	0.464	0.358	0.340
	r^2	0.9624	0.9624	0.9386
	χ^2	3.3206	4.3707	14.4918
Langmuir	$Q_{m(L)}$ (mg/g)	49.89	57.97	72.11
	K_L (L/mg)	0.016	0.031	0.043
	r^2	0.9813	0.9855	0.9931
	χ^2	1.6567	1.6844	1.6234
Temkin	K_T (L/g)	0.131	0.284	2.641
	E_T (J/mol)	212.77	200.70	259.29
	r^2	0.9806	0.9825	0.7832
	χ^2	1.7108	2.0394	11.2707
Dubinin-Radushkevich	$Q_{m(D-R)}$ (mg/g)	33.796	45.633	56.978
	E_{D-R} (kJ/mol)	0.067	0.095	0.157
	r^2	0.8997	0.9503	0.9050
	χ^2	8.8600	5.7794	22.4028

Table 3

The ΔG° , ΔH° , ΔS° values of the doripenem adsorption onto Alg@iB

Temperature (K)	Thermodynamic parameters		
	ΔG° (kJ/mol)	ΔH° (kJ/mol)	ΔS° (J/mol.K)
303	-22.204	40.09	206
313	-24.658		
323	-26.324		

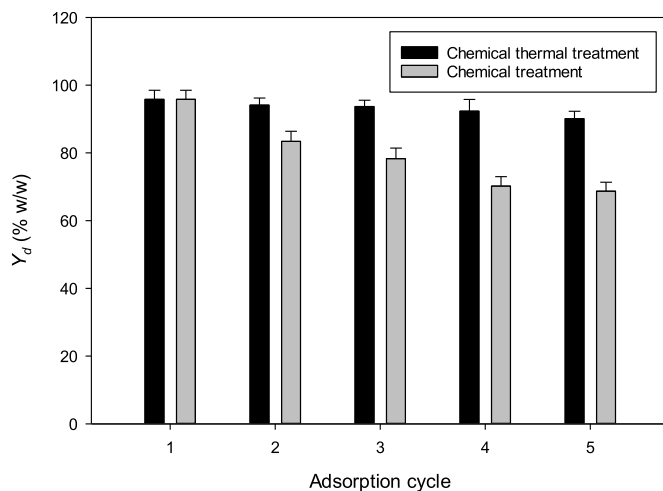


Fig. 7. The reusability study of Alg@iB in the removal of doripenem from the aqueous solution.

acid solution at room temperature, without heating. This suggests that the desorption of doripenem molecules from the surface of Alg@iB is endothermic, similar to its adsorption counterpart.

4. Conclusions

A low-cost bentonite-alginate (Alg@iB) composite beads with porous interior and high basal spacing have been successfully synthesized and used for efficient removal of doripenem from aqueous solution. The batch adsorption experiments show that high removal of doripenem can be achieved by Alg@iB, with the highest Y_d (95.8% w/w) monitored at pH = 5, $m_c = 1.4\%$ w/v, $T = 50$ °C, and $m_d = 250$ ppm. The study suggests that the adsorption of doripenem is spontaneous and endothermic, with the physical diffusion of doripenem from the bulk solution

to the boundary layer of Alg@iB as the rate-governing step, according to the multi-linear intra-particle diffusion (IPD) model. Moreover, the interaction between Alg@iB and doripenem is also observed to be driven by the chemical hydrogen binding. The reusability test shows that Alg@iB is stable until the fifth adsorption cycle. Therefore, this study suggests that Alg@iB can be employed as an efficient adsorbent for the removal of doripenem from the aqueous solution.

Declaration of competing interest

The authors declare that they have no known competing financial interests or personal relationships that could have appeared to influence the work reported in this paper.

Acknowledgement

This research did not receive any specific grant from funding agencies in the public, commercial, or not-for-profit sectors.

References

- Atkins, P., 1999. *Physical Chemistry, sixth ed.* Oxford University Press, London.
- Auta, M., Hameed, B.H., 2014. Chitosan-clay composite as highly effective and low-cost adsorbent for batch and fixed-bed adsorption of methylene blue. *Chem. Eng. J.* 237, 352–361. <https://doi.org/10.1016/j.cej.2013.09.066>.
- Blot, S., Antonelli, M., Arvaniti, K., Blot, K., Creagh-Brown, Ben, de Lange, D., De Waele, J., Deschepper, M., Dikmen, Y., Dimopoulos, G., Eckmann, C., Francois, G., Girardis, M., Koulenti, D., Labeau, S., Lipman, J., Lipovestky, F., Maseda, E., Montravers, P., Mikstacki, A., Paiva, J.A., Pereyra, C., Rello, J., Timsit, J.F., Vogelaers, D., Lamrous, A., Rezende-Neto, J., Cardenas, Y., Vymazal, T., Feldsoe-Nielsen, H., Kott, M., Kostoula, A., Javeri, Y., Einav, S., Makikado, L.D.U., Tomescu, D., Gritsan, A., Jovanovic, B., Venkatesan, K., Mirkovic, T., Creagh-Brown, Benedict, Lamrous, A., Emmerich, M., Canale, M., Dietz, L.S., Ilutovich, S., Miñope, J.T.S., Silva, R.B., Montenegro, M.A., Martin, P., Saul, P., Chediack, V., Sutton, G., Couce, R., Balasini, C., Gonzalez, S., Lascar, F.M., Descotte, E.J., Gumiel, N.S., Pino, C.A., Cesio, C., Valgolio, E., Cunto, E., Dominguez, C., Nelson, N.F., Abegao, E.M., Pozo, N.C., Bianchi, L., Correger, E., Pastorino, M.L., Miyazaki, E.A., Pozo, N.C., Grubisich, N., Garcia, M., Bonetto, N., Quevedo, N.E., Gomez, C.D., Queti, F., Estevearena, L.G., Fernandez, R., Santolaya, I., Pozo, N.C., Grangeat, S.H., Doglia, J., Zakalik, G., Pellegrini, C., Lloria, M.M., Chacon, M.E., Fumale, M., Leguizamón, M., Hidalgo, I.B., Tiranti, R.J., Capponi, P., Tita, A., Cardonnet, L., Bettini, L., Ramos, A., Lovesio, L., Miranda, E.M., Farfan, A.B., Tolosa, C., Segura, L., Bellocchio, A., Alvarez, B., Manzur, A., Lujan, R., Fernandez, N., Scarone, N., Zazu, A., Groh, C., Fletcher, J., Smith, J., Azad, R., Chavan, N., Wong, H., Kol, M., Campbell, L., Starr, T., Roberts, B., Wibrow, B., Warhurst, T., Chinthamunedi, M., Ferney, B.B., Simon, M., De Backer, D., Wittebole, X., De Bels, D., Collin, V., Dams, K., Jorens, P., Dubois, J., Gunst, J., Haentjens, L., De Schryver, N., Dugernier, T., Rezende-Neto, J., Rizoli, S., Santillan, P., Han, Y., Biskup, E., Qu, C., Li, X., Yu, T., Weihua, L., Molano-Franco, D., Rojas, J., Oviedo, J.M.P., Pinilla, D., Cardenas, Y., Celis, E., Arias, M., Vukovic, A., Vudrag, M., Belavic, M., Zunic, J., Kuharic, J., Kricka, I.B., Filipovic-Grcic, I., Tomasevic, B., Obraz, M., Budulica, B., Dohnal, M., Malaska, J., Kratochvil, M., Satinsky, I., Schwarz, P., Kos, Z., Blahut, L., Maca, J., Protus, M., Kieslichová, E., Nielsen, L.G., Krogh, B.M., Rivadeneira, F., Morales, F., Mora, J., Orozco, A.S., MorochoTutillo, D.R., Vargas, N.R., Yezpe, E.S., Villamagua, B., Alsi, A., Fahmy, A., Dupont, H., Lasocki, S., Paugam-Burtz, C., Foucrier, A., Nica, A., Barjon, G., Mallat, J., Marcotte, G., Leone, M., Duclos, G., Burtin, P., Atchade, E., Mahjoub, Y., Misset, B., Timsit, J.F., Dupuis, C., Veber, B., Debarre, M., Collange, O., Pottecher, J., Hecketsweiler, S., Fromentin, M., Tesnière, A., Koch, C., Sander, M., Kott, M., Elke, G., Wrigge, H., Simon, P., Chalkiadaki, A., Tzanidakis, C., Pneumatikos, I., Sertaridou, E., Mastora, Z., Pantazopoulos, I., Papanikolaou, M., Papavasiliopoulou, T., Floros, J., Kolonia, V., Diakaki, C., Rallis, M., Paridou, A., Kalogeromitros, A., Romanou, V., Nikolaou, C., Kounougeri, K., Tsigou, E., Psallida, V., Karampela, N., Mandragos, K., Kontoudaki, E., Pentheroudaki, A., Farazi-Chongouki, C., Karakosta, A., Chouris, I., Radu, V., Malliotakis, P., Kokkini, S., Charalambous, E., Kyritsi, A., Koulouras, V., Papanathanakos, G., Nagky, E., Lampiri, C., Tsimppoukas, F., Sarakatsanos, I., Georgakopoulos, P., Ravani, I., Prekates, A., Sakellaridis, K., Christopoulos, C., Vrettou, E., Stokkos, K., Pentari, A., Marmaridou, K., Kydonia, C., Tsoumaropoulos, G., Bitzani, M., Kontou, P., Voudouris, A., Elli-Nikki, Filoni, Antypa, E., Chasou, E., Anisoglou, S., Papageorgiou, E., Paraforou, T., Tsioka, A., Karathanou, A., Vavalos, A., Shah, B., Thakkar, C., Jain, N., Gurjar, M., Baronia, A., Sathe, P., Kulkarni, S., Paul, C., Paul, J., Masjedi, M., Nikandish, R., Zand, F., Sabetian, G., Mahmoodpour, A., Hashemian, S.M., Bala, M., Flocco, R., Torrente, S., Pota, V., Spadaro, S., Volta, C., Serafini, G., Boraso, S., Tiberio, I., Cortegiani, A., Misseri, G., Barbagallo, M., Nicolotti, D., Forfori, F., Corradi, F., De Pascale, G., Pelagalli, L., Brazzi, L., Vittone, F.G., Russo, A., Simion, D., Cotoia, A., Cinnella, G., Toppin, P., Johnson-Jackson, R., Hayashi, Y., Yamamoto, R., Yasuda, H., Kishihara, Y., Shiotsuka, J., Sanchez-Hurtado, L.A., Tejada-Huezo, B., Gorordo, L., Namendys-Silva, S.A., Garcia-Guillen, F.J., Martinez, M., Romero-Meja, E., Colorado-Dominguez, E., van den Oever, H., Kalff, K.M., Vermeijden, W., Cornet, A.D., Beck, O., Cimic, N., Dormans, T., Bormans, L., Bakker, J., Van Duijn, D., Bosman, G., Vos, P., Haas, L., Henein, A., Miranda, A.M., Makikado, L.D.U., Malca, G.E.G., Arroyo-Sanchez, A., Misiewska-Kaczur, A., Akinyi, F., Czuczwar, M., Luczak, K., Sulkowski, W., Tamowicz, B., Swit, B., Baranowski, B., Smuszkiewicz, P., Trojanowska, I., Rzymiski, S., Sawinski, M., Trosiak, M., Mikaszewska-Sokolewicz, M., Alves, R., Leal, D., Krystopchuk, A., Mendonca, P.M.H., Pereira, R.A., de Carvalho, M.R.L.M., Candeias, C., Molinos, E., Ferreira, Amélia, Castro, G., Pereira, J.M., Santos, L., Ferreira, Alcina, Pascoalinho, D., Ribeiro, R., Domingos, G., Gomes, P., Nora, D., Costa, R.P., Santos, A., Alsheikhly, A.S., Tomescu, D., Popescu, M., Grigoras, I., Patrascanu, E., Zabolotskikh, I., Musaeva, T., Gaigolnik, D., Kulabukhov, V., Belskiy, V., Zubareva, N., Tribulev, M., Abdelsalam, A., Aldarsani, A., Al-Khalid, M., Almekhlafi, G., Mandourah, Y., Jovanovic, B., Dokleštic, K., Velickovic, J., Velickovic, D., Jankovic, R., Vukovic, A., Skoric-Jokic, S., Radovanovic, D., Richards, G., Alli, A., del Carmen Cordoba Niefra, M., Iniesta, R.S., Martínez, A.B.C., Bernedo, C.G., Gil, S.A.P., Nuvalis, X., Garcia, J.G., Peña, J.M.G., Jimenez, R., Herrera, L., Barrachina, L.G., Monzon, I.C., Redondo, F.J., Villazala, R., Zapata, D.F.M., Lopez, I.M.V., Moreno-Gonzalez, G., Lopez-Delgado, J.C., Marin, J.S., Sanchez-Zamora, P., Vidal, M.V., González, J.F., Salinas, I., Hermosa, C., Martinez-Sagasti, F., Domingo-Marín, S., Victorino, J.A., Garcia-Alvarez, R., Calleja, P.L.A., de la Torre-Prados, M.V., Vidal-Cortes, P., del Río-Carbajo, L., Izura, J., Minguez, V., Alvarez, J. T., Prous, A.P., Paz, D., Roche-Campo, F., Aguilar, G., Belda, J., Rico-Feijoo, J., Aldecoa, C., Zalba-Etayo, B., Lang, M., Dullenkopf, A., Trongtrakul, K., Chitsomkasem, A., Akbas, T., Unal, M.N., Ozcelik, M., Gumus, A., Ramazanoglu, A., Memis, D., Mehmet, I., Urkmez, S., Ozgultekin, A., Demirkiran, O., Aslan, N.A., Kizilaslan, D., Kahveci, F., Ünlü, N., Ozkan, Z., Kaye, C., Jansen, J., O'Neill, O., Nutt, C., Jha, R., Hooker, N., Grecu, I., Petridou, C., Shyamsundar, M., McNamee, L., Trinder, J., Hagan, S., Kelly, C., Silversides, J., Groba, C.B., Boyd, O., Bhowmick, K., Humphreys, S., Summers, C., Polgarova, P., Margaron, M., Dickens, J., Pearson, S., Chinery, E., Hemmings, N., O'Kane, S., Austin, P., Cole, S., Plowright, C., Box, R., Wright, C., Young, L., Montague, L., Parker, R., Morton, B., Ostermann, M., Bilinska, J., Rose, B.O., Reece-Anthony, R., Ryan, C., Hamilton, M., Hopkins, P., Wendon, J., Brescia, G., Ijaz, N., Wood, J., George, M., Toth-Tarsoly, P., Yates, B., Armstrong, M., Scott, C., Boyd, C., Szakmany, T., Rees, D., Pulak, P., Coggon, M., Saha, B., Kent, L., Gibson, B., Camsooksai, J., Reschreiter, H., Morgan, P., Sangaralingham, S., Lowe, A., Vondras, P., Jamadarkhana, S., Cruz, C., Bhandary, R., Hersey, P., Furneal, J., Innes, R., Doble, P., Attard, C.B., Parsons, P., Page, V., Zhao, X., Grecu, I., Dalton, J., Hegazy, M., Awad, Y., Naylor, D., Naylor, A., Lee, S., Brevard, S., Davis, N., 2019. Epidemiology of intra-abdominal infection and sepsis in critically ill patients: "AbSeS", a multinational observational cohort study and ESICM Trials Group Project. *Intensive Care Med.* 45, 1703–1717. <https://doi.org/10.1007/s00134-019-05819-3>.
- Blot, S., De Waele, J.J., 2005. Critical issues in the clinical management of complicated intra-abdominal infections. *Drugs* 65, 1611–1620. <https://doi.org/10.2165/00003495-200565120-00002>.
- Chen, Y., Duan, H., Zhu, C., Ye, W., Sun, Y., Wu, D., 2012. Adsorption of La(III) onto GMZ bentonite: effect of contact time, bentonite content, pH value and ionic strength. *J. Radioanal. Nucl. Chem.* 292, 1339–1347. <https://doi.org/10.1007/s10967-012-1612-6>.
- Chowdhury, S., Mishra, R., Saha, P., Kushwaha, P., 2011. Adsorption thermodynamics, kinetics and isosteric heat of adsorption of malachite green onto chemically modified rice husk. *Desalination* 265, 159–168. <https://doi.org/10.1016/j.desal.2010.07.047>.
- Ely, A., Baudu, M., Basly, J.P., Kankou, M.O.S.A.O., 2009. Copper and nitrophenol pollutants removal by Na-montmorillonite/alginate microcapsules. *J. Hazard Mater.* 171, 405–409. <https://doi.org/10.1016/j.jhazmat.2009.06.015>.
- Fabryanty, R., Valencia, C., Soetaredjo, F.E., Putro, J.N., Santoso, S.P., Kurniawan, A., Ju, Y.H., Ismadij, S., 2017. Removal of crystal violet dye by adsorption using bentonite – alginate composite. *J. Environ. Chem. Eng.* 5, 5677–5687. <https://doi.org/10.1016/j.jece.2017.10.057>.
- Fu, H., Li, X., Wang, J., Lin, P., Chen, C., Zhang, X., Suffet, I.H., 2017. Activated carbon adsorption of quinolone antibiotics in water: performance, mechanism, and modeling. *J. Environ. Sci. (China)* 56, 145–152. <https://doi.org/10.1016/j.jes.2016.09.010>.
- Gao, Y., Li, Y., Zhang, L., Huang, H., Hu, J., Shah, S.M., Su, X., 2012. Adsorption and removal of tetracycline antibiotics from aqueous solution by graphene oxide. *J. Colloid Interface Sci.* 368, 540–546. <https://doi.org/10.1016/j.jcis.2011.11.015>.
- Genç, N., Dogan, E.C., Yurtsever, M., 2013. Bentonite for ciprofloxacin removal from aqueous solution. *Water Sci. Technol.* 68, 848–855. <https://doi.org/10.2166/wst.2013.313>.
- Greer, N.D., 2008. Doripenem (Doribax): the newest addition to the carbapenems. *Baylor Univ. Med. Cent. Proc.* 21, 337–341. <https://doi.org/10.1080/08998280.2008.11928422>.
- Hilas, O., Ezzo, D.C., Jodlowski, T.Z., 2008. Doripenem (Doribax), a new carbapenem antibacterial agent. *P T* 33, 134–137.
- Ho, Y.S., McKay, G., 1999. Pseudo-second order model for sorption processes. *Process Biochem.* 34, 451–465.
- Huber, M.M., Göbel, A., Joss, A., Hermann, N., Löffler, D., McArdell, C.S., Ried, A., Siegrist, H., Ternes, T.A., Von Gunten, U., 2005. Oxidation of pharmaceuticals during ozonation of municipal wastewater effluents: a pilot study. *Environ. Sci. Technol.* <https://doi.org/10.1021/es048396s>.
- Košutić, K., Dolar, D., Ašperger, D., Kunst, B., 2007. Removal of antibiotics from a model wastewater by RO/NF membranes. *Separ. Purif. Technol.* 53, 244–249. <https://doi.org/10.1016/j.seppur.2006.07.015>.
- Liu, Y., Liu, Y.J., 2008. Biosorption isotherms, kinetics and thermodynamics. *Separ. Purif. Technol.* 61, 229–242. <https://doi.org/10.1016/j.seppur.2007.10.002>.

- Maged, A., Kharbush, S., Ismael, I.S., Bhatnagar, A., 2020. Characterization of activated bentonite clay mineral and the mechanisms underlying its sorption for ciprofloxacin from aqueous solution. *Environ. Sci. Pollut. Res.* 27, 32980–32997. <https://doi.org/10.1007/s11356-020-09267-1>.
- Mazzei, T., 2010. The pharmacokinetics and pharmacodynamics of the carbapenems: focus on doripenem. *J. Chemother.* 22, 219–225. <https://doi.org/10.1179/joc.2010.22.4.219>.
- Mousavi, S.A., Janjani, H., 2020. Antibiotics adsorption from aqueous solutions using carbon nanotubes: a systematic review. *Toxin Rev.* 39, 87–98. <https://doi.org/10.1080/15569543.2018.1483405>.
- Pawar, R.R., Gupta, P., Lalhmunsiam Bajaj, H.C., Lee, S.M., 2016. Al-intercalated acid activated bentonite beads for the removal of aqueous phosphate. *Sci. Total Environ.* 572, 1222–1230. <https://doi.org/10.1016/j.scitotenv.2016.08.040>.
- Pawar, R.R., Lalhmunsiam Ingole, P.G., Lee, S.M., 2020. Use of activated bentonite-alginate composite beads for efficient removal of toxic Cu²⁺ and Pb²⁺ ions from aquatic environment. *Int. J. Biol. Macromol.* 164, 3145–3154. <https://doi.org/10.1016/j.ijbiomac.2020.08.130>.
- Peng, B., Chen, L., Que, C., Yang, K., Deng, F., Deng, X., Shi, G., Xu, G., Wu, M., 2016. Adsorption of antibiotics on graphene and biochar in aqueous solutions induced by π - π interactions. *Sci. Rep.* <https://doi.org/10.1038/srep31920>.
- Rusmin, R., Sarkar, B., Liu, Y., McClure, S., Naidu, R., 2015. Structural evolution of chitosan-palygorskite composites and removal of aqueous lead by composite beads. *Appl. Surf. Sci.* 353, 363–375. <https://doi.org/10.1016/j.apsusc.2015.06.124>.
- Sakr, Y., Jaschinski, U., Wittebole, X., Szakmany, T., Lipman, J., Namendys-Silva, S.A., Martin-Loeches, I., Leone, M., Lupu, M.N., Vincent, J.L., 2018. Sepsis in intensive care unit patients: worldwide data from the intensive care over nations audit. *Open Forum Infect. Dis.* 5, 1–9. <https://doi.org/10.1093/ofid/ofy313>.
- Santoso, S.P., Angkawijaya, A.E., Yuliana, M., Bundjaja, V., Soetaredjo, F.E., Ismadji, S., Go, A.W., Tran-Nguyen, P.L., Kurniawan, A., Ju, Y.H., 2020. Saponin-intercalated organoclays for adsorptive removal of β -carotene: equilibrium, reusability, and phytotoxicity assessment. *J. Taiwan Inst. Chem. Eng.* <https://doi.org/10.1016/j.jtice.2020.11.036>.
- Sartelli, M., Chichom-Mefire, A., Labricciosa, F.M., Hardcastle, T., Abu-Zidan, F.M., Adesunkanmi, A.K., Ansaloni, L., Bala, M., Balogh, Z.J., Beltrán, M.A., Ben-Ishay, O., Biffi, W.L., Birindelli, A., Cainzos, M.A., Catalini, G., Ceresoli, M., Che Jusoh, A., Chiara, O., Coccolini, F., Coimbra, R., Cortese, F., Demetrashevili, Z., Di Saverio, S., Diaz, J.J., Egiev, V.N., Ferrada, P., Fraga, G.P., Ghnam, W.M., Lee, J.G., Gomes, C. A., Hecker, A., Herzog, T., Kim, J. I., Inaba, K., Isik, A., Karamarkovic, A., Kashuk, J., Khokha, V., Kirkpatrick, A.W., Kluger, Y., Koike, K., Kong, V.Y., Leppaniemi, A., Machain, G.M., Maier, R.V., Marwah, S., McFarlane, M.E., Montori, G., Moore, E.E., Negoi, I., Olaoye, I., Omari, A.H., Ordóñez, C.A., Pereira, B.M., Pereira Júnior, G.A., Pupelis, G., Reis, T., Sakakhushev, B., Sato, N., Segovia Lohse, H.A., Shelat, V.G., Søreide, K., Uhl, W., Ulrych, J., Van Goor, H., Velmahos, G.C., Yuan, K.C., Wani, I., Weber, D.G., Zachariah, S.K., Catena, F., 2017. The management of intra-abdominal infections from a global perspective: 2017 WSES guidelines for management of intra-abdominal infections. *World J. Emerg. Surg.* 12, 3–34. <https://doi.org/10.1186/s13017-017-0141-6>.
- Shyam, R., Puri, J.K., Kaur, H., Amutha, R., Kapila, A., 2013. Single and binary adsorption of heavy metals on fly ash samples from aqueous solution. *J. Mol. Liq.* 178, 31–36. <https://doi.org/10.1016/j.molliq.2012.10.031>.
- Simon, M.A., Anggraeni, E., Soetaredjo, F.E., Santoso, S.P., Irawaty, W., Thanh, T.C., Hartono, S.B., Yuliana, M., Ismadji, S., 2019. Hydrothermal synthesis of HF-free MIL-100(Fe) for isoniazid-drug delivery. *Sci. Rep.* 9, 1–11. <https://doi.org/10.1038/s41598-019-53436-3>.
- Tan, W.S., Ting, A.S.Y., 2014. Alginate-immobilized bentonite clay: adsorption efficacy and reusability for Cu(II) removal from aqueous solution. *Bioresour. Technol.* 160, 115–118. <https://doi.org/10.1016/j.biortech.2013.12.056>.
- Ternes, T., Joss, A., Siegrist, H., 2004. Peer reviewed: scrutinizing pharmaceuticals and personal care products in wastewater treatment. *Environ. Sci. Technol.* 38, 392A–399A.
- Tonucci, M.C., Gurgel, L.V.A., Aquino, S.F. de, 2015. Activated carbons from agricultural byproducts (pine tree and coconut shell), coal, and carbon nanotubes as adsorbents for removal of sulfamethoxazole from spiked aqueous solutions: kinetic and thermodynamic studies. *Ind. Crop. Prod.* 74, 111–121. <https://doi.org/10.1016/j.indcrop.2015.05.003>.
- Vincent, J., Marshall, J., Anzueto, A., Martin, C.D., Gomersall, C., 2016. International study of the prevalence and outcomes of infection in Intensive Care Units. *J. Am. Med. Assoc.* 302, 2323–2329.
- Wang, Y., Gong, S., Li, Y., Li, Z., Fu, J., 2020. Adsorptive removal of tetracycline by sustainable ceramsite substrate from bentonite/red mud/pine sawdust. *Sci. Rep.* 10, 1–18. <https://doi.org/10.1038/s41598-020-59850-2>.
- Widyaningsih, L., Setiawan, A., Santoso, S.P., Soetaredjo, F.E., Ismadji, S., Hartono, S. B., Ju, Y.H., Tran-Nguyen, P.L., Yuliana, M., 2020. Feasibility study of nanocrystalline cellulose as adsorbent of steryl glucosides from palm-based biodiesel. *Renew. Energy* 154, 99–106. <https://doi.org/10.1016/j.renene.2020.03.001>.
- Xu, X., Wang, B., Tang, H., Jin, Z., Mao, Y., Huang, T., 2020. Removal of phosphate from wastewater by modified bentonite entrapped in Ca-alginate beads. *J. Environ. Manag.* 260 <https://doi.org/10.1016/j.jenvman.2020.110130>.
- Yu, J., Kang, Y., Yin, W., Fan, J., Guo, Z., 2020. Removal of antibiotics from aqueous solutions by a carbon adsorbent derived from protein-waste-doped biomass. *ACS Omega* 5. <https://doi.org/10.1021/acsomega.0c02568>, 19187–19193.
- Zeng, Z.W., Tan, X.F., Liu, Y.G., Tian, S.R., Zeng, G.M., Jiang, L.H., Liu, S.B., Li, J., Liu, N., Yin, Z.H., 2018. Comprehensive adsorption studies of doxycycline and ciprofloxacin antibiotics by biochars prepared at different temperatures. *Front. Chem.* 6, 1–11. <https://doi.org/10.3389/fchem.2018.00080>.